The Journal of Chemical Physics

Density-inversion method for the Kohn–Sham potential: Role of the screening density

Cite as: J. Chem. Phys. **152**, 164114 (2020); https://doi.org/10.1063/5.0005781
Submitted: 25 February 2020 . Accepted: 07 April 2020 . Published Online: 29 April 2020

Timothy J. Callow, Nektarios N. Lathiotakis, and Nikitas I. Gidopoulos

The Journal of Chemical Physics ARTICLE scitation.org/journal/jcp

Density-inversion method for the Kohn–Sham potential: Role of the screening density

Cite as: J. Chem. Phys. 152, 164114 (2020); doi: 10.1063/5.0005781
Submitted: 25 February 2020 • Accepted: 7 April 2020 •
Published Online: 29 April 2020

Timothy J. Callow,[1,2,a)] Nektarios N. Lathiotakis,[3,b)] and Nikitas I. Gidopoulos[1,c)]

AFFILIATIONS

[1] Department of Physics, Durham University, South Road, Durham DH1 3LE, United Kingdom
[2] Max-Planck-Institut für Mikrostrukturphysik, Weinberg 2, D-06120 Halle, Germany
[3] Theoretical and Physical Chemistry Institute, National Hellenic Research Foundation, Vass. Constantinou 48, 116 35 Athens, Greece

[a)] **Electronic mail:** timothy.callow@durham.ac.uk
[b)] **Electronic mail:** lathiot@eie.gr
[c)] **Author to whom correspondence should be addressed:** nikitas.gidopoulos@durham.ac.uk

ABSTRACT

We present a method to invert a given density and find the Kohn–Sham (KS) potential in Density Functional Theory (DFT) that shares the density. Our method employs the concept of screening density, which is naturally constrained by the inversion procedure and thus ensures that the density being inverted leads to a smooth KS potential with correct asymptotic behavior. We demonstrate the applicability of our method by inverting both local and non-local (Hartree–Fock and coupled cluster) densities; we also show how the method can be used to mitigate the effects of self-interactions in common DFT potentials with appropriate constraints on the screening density.

I. INTRODUCTION

Density functional theory (DFT) is the most widely used method in electronic structure theory calculations, with many tens of thousands of publications using it every year.[1] Despite the many successes of the Kohn–Sham (KS) formalism in DFT, the most commonly used functionals do not correctly describe various physical situations, such as molecular dissociation and charge transfer processes.[2,3] Developing methods to overcome these difficulties is an active area of research.[4–9]

In order to judge the quality of new approaches in KS theory, it is important to have an accurate reference against which to benchmark results. Often, we can compare with an experiment or a higher level calculation; however, it is also valuable to know what an "exact" KS result is. This is commonly done by inverting an accurate density to find the corresponding KS potential. Various methods have been developed to accurately obtain the KS potential from a given density. Early attempts typically focused on small atomic systems;[10–17] more generally applicable methods,[18–24] including the time-dependent case,[25–27] have subsequently been developed. However, the problem remains interesting due to its associated difficulties.[28]

In this paper, we present a method[29] to invert a known target density ρ_t of a system of N interacting electrons in a known external potential $v_{\rm en}$, in order to obtain the Hartree-exchange and correlation (Hxc) potential of the KS system with density ρ_t. Our method is based on minimizing the Coulomb energy $U[\rho_v - \rho_t]$ of the density difference $\rho_v - \rho_t$,

$$U[\rho_v - \rho_t] = \frac{1}{2}\iint \mathrm{d}\mathbf{r}\,\mathrm{d}\mathbf{r}'\,\frac{[\rho_v(\mathbf{r}) - \rho_t(\mathbf{r})][\rho_v(\mathbf{r}') - \rho_t(\mathbf{r}')]}{|\mathbf{r} - \mathbf{r}'|}, \quad (1)$$

where ρ_v is the density of another noninteracting N-electron system with KS potential $v_{\rm en} + v$. Obviously, the effective potential v simulates the electronic repulsion, and at the minimum of the Coulomb energy U, when $\rho_v = \rho_t$, this effective potential becomes equal to the Hxc potential we seek.[30]

The Coulomb energy U is clearly positive and tends to zero as the two densities become close to each other. As will be explained in Sec. II, minimizing U also minimizes the energy difference

from Ref. 31,

$$T_\Psi[v] = \langle \Psi | H_v | \Psi \rangle - E_v, \tag{2}$$

where Ψ is a state with density ρ_t, and H_v is the many-body KS Hamiltonian,

$$H_v = \sum_{i=1}^{N} \left[-\frac{\nabla_i^2}{2} + v_{\text{en}}(\mathbf{r}_i) + v(\mathbf{r}_i) \right], \tag{3}$$

of the KS system with density ρ_v. When Ψ is the (exact or approximate) ground state of the interacting system in the external potential v_{en}, the minimizing potential of Eqs. (1) and (2) will be (exactly or approximately) equal to the Hxc potential of the KS system with density ρ_t.

Central to our method is the concept of screening density,[32] or electron repulsion density,[6] in the KS scheme. It can be thought of as the effective electron density that screens the nuclear charge from a KS electron (i.e., electron in a KS orbital). Alternatively, it is the effective charge density that repels each KS electron, mimicking the electron–electron repulsion and underpinning the Hartree, exchange and correlation (Hxc) potential. Specifically, using Poisson's equation, the screening density can be obtained from the Laplacian of the Hxc potential, $\rho_{\text{scr}}(\mathbf{r}) = -(1/4\pi)\,\nabla^2 v_{\text{Hxc}}(\mathbf{r})$.[6,32] Görling[33] and Liu, Ayers, and Parr[34] had previously considered the xc-only screening density, obtained from the Laplacian of the xc-potential.

In our algorithm for density inversion, the screening charge (the integral of the screening density over all space) is fixed; this stabilizes the minimization procedure and means we can constrain our potentials to be smooth and have the correct asymptotic behavior, as we shall see that multiple potentials can arise from the inversion of the same density. Inverting DFT densities under appropriate constraints for the screening charge also provides a reliable procedure for alleviating self-interaction errors[35] in common DFT functionals.

The paper is structured as follows: In Sec. II, we demonstrate the algorithm used to minimize (1). In Sec. III, we first demonstrate the accuracy and applicability of our method by inverting local-density approximation (LDA) densities for several molecules. We also show how inverting LDA densities under a constraint for the screening charge yields LDA potentials with self-interaction errors largely corrected. We then demonstrate how it can be applied to Hartree–Fock (HF) and coupled cluster densities to obtain accurate exchange-only and xc-potentials. Finally, we draw a brief comparison with the density inversion method of Zhao, Morrison, and Parr,[19] which uses the objective functional in Eq. (1) in a different manner.

II. METHOD

In order to minimize the objective functional in (1), we split the KS potential into the electron-nuclear part and an effective potential $v(\mathbf{r})$. At the minimum, the effective potential will coincide with the Hxc potential we seek, for the KS system with density $\rho_t(\mathbf{r})$. We represent the effective potential $v(\mathbf{r})$ using a *screening* density as follows:[32]

$$v_s(\mathbf{r}) = v_{\text{en}}(\mathbf{r}) + v(\mathbf{r}), \tag{4}$$

$$v(\mathbf{r}) = \int d\mathbf{r}' \frac{\rho_{\text{scr}}(\mathbf{r}')}{|\mathbf{r} - \mathbf{r}'|}. \tag{5}$$

This is always a valid representation for the potential due to Poisson's law.[33] The screening density integrates to a screening charge Q_{scr},

$$\int d\mathbf{r} \rho_{\text{scr}}(\mathbf{r}) = Q_{\text{scr}}, \tag{6}$$

with

$$N - 1 \le Q_{\text{scr}} \le N. \tag{7}$$

We argue that the value of Q_{scr} is a measure of self-interactions (SIs):[32] $Q_{\text{scr}} = N - 1$ is a necessary condition for a method to be fully self-interaction free; otherwise, the method is contaminated with self-interactions. As the value of Q_{scr} does not change in the implementation of the method that we will describe, it is important to start with a screening density that is consistent with the screening charge of the target density.

When we vary $v(\mathbf{r})$ as $v(\mathbf{r}) \to v(\mathbf{r}) + \epsilon\ \delta v(\mathbf{r})$, with $\delta v(\mathbf{r}) = \int d\mathbf{r}' \delta\rho_{\text{scr}}(\mathbf{r}')/|\mathbf{r} - \mathbf{r}'|$, the change in the Coulomb energy U (functional of v) is given by

$$\delta U[v] = \epsilon \iint d\mathbf{r}\, d\mathbf{r}' \delta\rho_{\text{scr}}(\mathbf{r}) \tilde{\chi}_v(\mathbf{r}, \mathbf{r}') \delta\rho(\mathbf{r}') + \mathcal{O}(\epsilon^2), \tag{8}$$

with

$$\delta\rho(\mathbf{r}) = \rho_v(\mathbf{r}) - \rho_t(\mathbf{r}) \tag{9}$$

and

$$\tilde{\chi}_v(\mathbf{r}, \mathbf{r}') = \iint d\mathbf{x}\, d\mathbf{y} \frac{\chi_v(\mathbf{x}, \mathbf{y})}{|\mathbf{r} - \mathbf{x}||\mathbf{r}' - \mathbf{y}|}, \tag{10}$$

where $\chi_v(\mathbf{r}, \mathbf{r}')$ is the density–density response function for the KS system,

$$\chi_v(\mathbf{r}, \mathbf{r}') = \sum_i^{\text{occ}} \sum_a^{\text{unocc}} \frac{\phi_{v,i}(\mathbf{r}) \phi_{v,a}^*(\mathbf{r}) \phi_{v,i}^*(\mathbf{r}') \phi_{v,a}(\mathbf{r}')}{\epsilon_{v,i} - \epsilon_{v,a}} + \text{c.c.}, \tag{11}$$

where $\phi_{v,i}$, $\phi_{v,a}$ and $\epsilon_{v,i}$, $\epsilon_{v,a}$ are the occupied and unoccupied KS orbitals and their KS eigenvalues in the KS determinant with density ρ_v [the ground state of H_v in (3)].

Since $\chi_v(\mathbf{r}, \mathbf{r}')$ is a negative-semidefinite operator, if we vary $\rho_{\text{scr}}(\mathbf{r})$ in the direction

$$\rho_{\text{scr}}(\mathbf{r}) \to \rho_{\text{scr}}(\mathbf{r}) + \epsilon\delta\rho(\mathbf{r}), \text{ with } \epsilon > 0, \tag{12}$$

then U will decrease. We can therefore use a gradient-descent method to minimize U. This minimization will also ensure that the quantity $T_\Psi[v]$ in (2) is minimized, since the functional derivative of $T_\Psi[v]$[31] is equal to $-\delta\rho(\mathbf{r})$, when $\rho_t(\mathbf{r})$ is the density of Ψ.

We note that during the minimization procedure, the screening charge Q_{scr} remains equal to the value of the initial guess for $\rho_{\text{scr}}(\mathbf{r})$, since $\int d\mathbf{r}\, \delta\rho(\mathbf{r}) = 0$.

A. Algorithm

The method has been implemented in the Gaussian basis set code HIPPO,[36] with one- and two-electron integrals for the Cartesian Gaussian basis elements calculated using the Gamess code.[61,62] The algorithm is described below.

1. Initialize the screening density as follows:

$$\rho_{\text{scr}}^{(0)}(\mathbf{r}) = \frac{N - \alpha}{N} \rho^{(0)}(\mathbf{r}), \tag{13}$$

where $\alpha \in [0, 1]$ depends on the target density, and thus, $Q_{scr} = N - \alpha$. $\rho^0(\mathbf{r})$ can be any density for the N-electron system.

$\rho_{scr}(\mathbf{r})$ is expanded in an auxiliary basis set as follows:

$$\rho_{scr}(\mathbf{r}) = \sum_k \rho_k^s \theta_k(\mathbf{r}). \tag{14}$$

For our auxiliary basis, we employed the density-fitted basis set[37] corresponding to the orbital basis. Justification for this choice of auxiliary set is given in Appendix A.

2. Solve the single-particle KS equations

$$\left[-\frac{\nabla^2}{2} + v_{en}(\mathbf{r}) + v(\mathbf{r})\right]\phi_{v,i}(\mathbf{r}) = \epsilon_{v,i}\,\phi_{v,i}(\mathbf{r}) \tag{15}$$

to update the density $\rho_v(\mathbf{r})$.

3. Update the screening density of the ith iteration in the direction

$$\delta\rho_{scr}^{(i)}(\mathbf{r}) = \epsilon\left[\rho_v^{(i)}(\mathbf{r}) - \rho_t(\mathbf{r})\right], \tag{16}$$

where ϵ is chosen with a quadratic line search to minimize U.

At this step, it is convenient for the target density to be expanded in the same basis set as the KS density $\rho_v(\mathbf{r})$, since the density difference is thus directly obtained.

4. Repeat steps 2 and 3 until either
   i. U and δU are converged to within some chosen tolerances, or
   ii. the amount and rate of increase in *negative* screening charge $Q_{neg} \geq 0$ exceeds a chosen amount, where

$$Q_{neg} = \frac{1}{2}\left[\int d\mathbf{r}|\rho_{scr}(\mathbf{r})| - Q_{scr}\right]. \tag{17}$$

Condition 4.ii. is a kind of regularization.[28,38] Due to both numerical issues (such as the effect of finite basis sets[39–41]) and possible theoretical constraints (non-interacting v-representability[42–47]), converging U to within the above tolerances can lead to spurious oscillations in the potential. This behavior frequently coincides with a large build-up of negative screening charge, and thus, a simple criterion to avoid these scenarios is to stop the procedure when this occurs. Details of the convergence criteria used can be found in Appendix B.

III. RESULTS

A. Inversion of LDA densities

To demonstrate the applicability of our method, we first present results for the inversion of LDA densities for a few atomic and molecular systems. As previously discussed, it is important to begin with the correct Q_{scr} for the system under consideration. As can be seen in Fig. 1, minimizing $U[\rho_v - \rho_t]$ for the same target density yields a unique potential for every value of Q_{scr}. Obviously, only the potential with the correct Q_{scr} will yield the target density ρ_t exactly.

Since LDA potentials are contaminated with self-interactions, we would expect physically that $Q_{scr} = N$ in this case. However, this turns out not to be true when we transform from a grid representation for the LDA xc-potential (as is typical in most codes) to the representation given by Eqs. (5) and (14). We observe that, in this

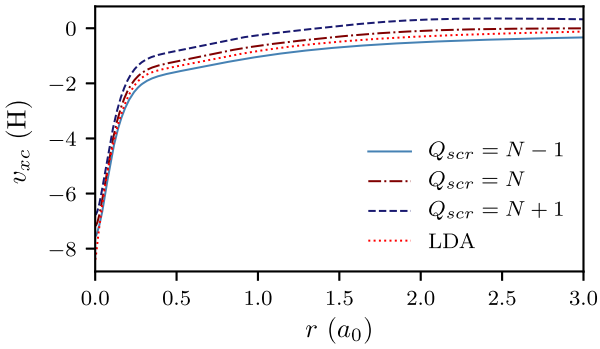

FIG. 1. The inverted xc-potentials from the LDA density of neon (cc-pVTZ), for different values of Q_{scr}. Each value of Q_{scr} produces a unique xc-potential.

representation, $Q_{scr} \neq N$ and is basis-set dependent. To determine the value of Q_{scr}, we solve the equation

$$\rho_k^{xc} = \sum_l \langle\tilde{\theta}_k|\theta_l\rangle^{-1}\langle\theta_l|v_{xc}\rangle \tag{18}$$

with

$$\rho_{xc}(\mathbf{r}) = \sum_k \rho_k^{xc}\theta_k(\mathbf{r}), \quad \tilde{\theta}_k(\mathbf{r}) = \int d\mathbf{r}'\frac{\theta_k(\mathbf{r}')}{|\mathbf{r} - \mathbf{r}'|}. \tag{19}$$

Here, $\rho_{xc}(\mathbf{r})$ is the effective xc-screening density, with $\int d\mathbf{r}\,\rho_{xc}(\mathbf{r}) = -\alpha$. Table I shows some values of Q_{scr} for helium and beryllium with an increase in the basis set size.

If desired, it is possible to approach $Q_{scr} = N$ by adding diffuse s-functions to the auxiliary basis set. As this affects the potential only by a small amount in the asymptotic tail, we choose not to modify the established basis sets in this work.

With a method to calculate the appropriate value of Q_{scr} for LDA densities, we now demonstrate the accuracy of our method when applied to LDA densities and the convergence with an increase in the basis set size. In Fig. 2, we see the qualitative similarities between the xc-potential from the inverted LDA density, and the actual LDA xc-potential. The region of biggest difference is observed near the nuclei; if accuracy in this region is desired, it is important to use a large basis set.

We can also use the HOMO energy as an indicator of the quality of the inversion procedure. In Table II, we present results for the percentage difference between the actual and inverted HOMO energy for some atoms and molecules. These results demonstrate

TABLE I. Values of α, where $Q_{scr} = N - \alpha$, and ionization potentials (IPs) as the negative of the HOMO energies, for He and Be with an increase in the basis set size. Basis sets are from Ref. 48.

	He		Be	
	α	IP (eV)	α	IP (eV)
cc-pVDZ	0.479	15.15	0.207	4.50
cc-pVTZ	0.214	14.82	0.148	4.81
cc-pVQZ	0.301	15.41	0.185	5.29
cc-pV5Z	0.256	15.89	0.165	5.41

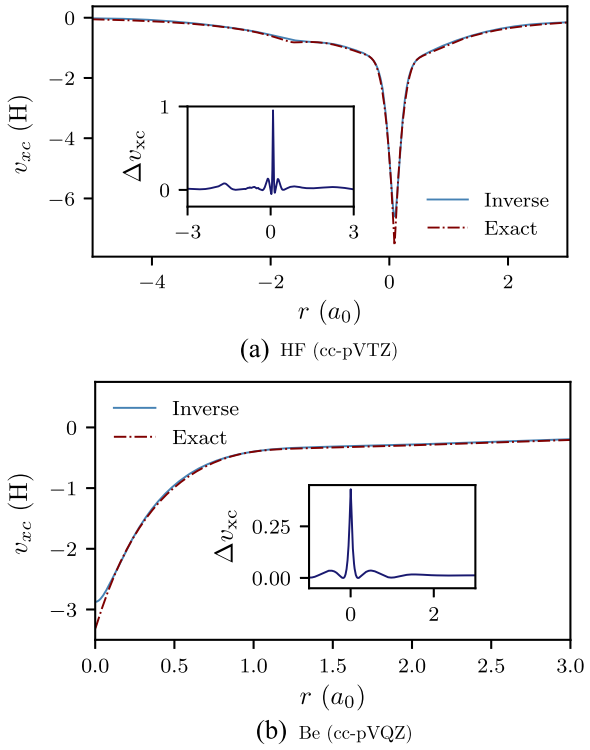

FIG. 2. Comparison of xc-potentials for the inverted LDA density and the exact LDA result.

the improved accuracy with respect to the basis set size, as well as a rough indication of how accurate we can expect our potentials to be with a given basis set.

B. Constrained LDA results

In Subsection III A, we demonstrated the importance of choosing the right screening charge when inverting LDA densities. However, the flexibility we have in choosing the screening charge can be used to our advantage, to remove the effects of self-interactions (SIs) from LDA and other SI contaminated densities by setting $Q_{\text{scr}} = N - 1$. The success of this "constrained DFT" approach has already been demonstrated,[6,32] but using a different method in which the energy is minimized under the following constraints:

$$Q_{\text{scr}} = N - 1, \tag{20}$$

and

$$\rho_{\text{scr}}(\mathbf{r}) \geq 0. \tag{21}$$

The second constraint (21) is an approximation, which in the aforementioned method is required to prevent a negative screening charge "hole" localizing at infinity. In our density inversion approach, we have employed the weaker condition 4.ii. (17) instead of (21).

In Table III, we see a comparison of the ionization potentials (IPs), taken to be the negative of the HOMO orbital energies.[49] We see that inverting the density under the constraint $Q_{\text{scr}} = N - 1$ and our previous constrained-LDA (CLDA) method[32] with the positivity constraint both yield very similar results for the IPs. As discussed in earlier work and seen here, this constrained method yields consistently better IPs than normal LDA, but preserves the energetics from the LDA calculation. Further analysis of the tendency for $\rho_{\text{scr}}(\mathbf{r})$ to be positive can be found in Appendix A.

TABLE III. Comparison of IPs (from HOMO energies) for constrained-LDA using the inversion of density and our previous CLDA method.[32] All basis sets are cc-pVTZ.

	LDA	CLDA (inv.)	CLDA[32]	Expt.[50]
He	15.47	23.12	23.82	24.59
Be	5.60	8.48	8.65	9.32
Ne	13.17	18.85	18.89	21.56
HF	9.38	14.08	14.17	16.03
H_2O	6.83	11.10	11.04	12.62
H_2	10.25	15.15	15.64	15.43
CO	8.97	12.50	12.84	14.01

C. Inversion of "non-local" densities

The principal application of the density inversion scheme is to invert densities obtained with non-DFT methods to find the KS potential that shares the same density. We have applied our

TABLE II. Comparison of IPs (from HOMO energies) of the inverted LDA densities with the actual LDA IPs.

	cc-pVDZ			cc-pVTZ			cc-pVQZ		
IP (eV)	Inverse	LDA	% err.	Inverse	LDA	% err.	Inverse	LDA	% err.
He	15.15	15.14	0.1	14.82	15.47	4.2	15.41	15.37	0.6
Be	4.50	5.62	19.9	4.81	5.60	14.1	5.29	5.60	5.5
Ne	6.69	12.24	45.3	10.56	13.17	19.8	11.75	13.40	12.3
HF	7.18	8.45	15.0	8.91	9.38	5.0	9.37	9.64	2.8
H_2O	5.71	6.23	8.3	6.67	7.00	4.7	6.86	7.21	4.4
H_2	9.53	10.12	5.8	10.00	10.25	2.4	10.02	10.26	2.3
CO	6.16	8.71	29.3	7.73	9.07	14.8	8.82	9.11	3.2
Avg % err.	...	...	17.7	...	...	9.3	...	...	4.5

TABLE IV. Comparison of IPs for the local potential of an HF density with the actual HF IPs.

	cc-pVDZ			cc-pVTZ			cc-pVQZ		
IP (eV)	Inverse	HF	% err.	Inverse	HF	% err.	Inverse	HF	% err.
He	25.23	24.88	1.4	24.97	24.97	0.0	24.98	24.98	0.0
Be	8.96	8.41	6.5	8.42	8.42	0.0	8.37	8.42	0.6
Ne	17.57	22.65	22.4	22.19	23.01	3.6	24.40	23.10	5.6
HF	14.21	17.12	17.0	16.57	17.52	5.4	17.23	17.64	2.3
H_2O	12.03	13.44	10.5	12.99	13.76	5.6	13.40	13.85	3.2
H_2	16.13	16.10	0.2	16.16	16.16	0.0	16.17	16.17	0.0
CO	11.65	14.96	22.1	13.74	15.09	8.9	14.03	15.11	7.1
Avg % err.	...	...	11.5	...	...	3.4	...	...	2.7

scheme to two densities calculated with Hartree–Fock (HF) and Coupled Cluster Singles Doubles (Triples) [CCSD(T)] theories, with target CCSD(T) densities obtained from the PSI4 code.[51,52] We focus on these because the inversion of an HF density gives us an exchange-only local potential in DFT [local Fock exchange (LFX)[29]], which is a close approximation to the exact-exchange potential.[29,53] CCSD(T) calculations yield highly accurate densities,[54] which give us an idea of what the "exact" xc-potential in KS theory should be.

Just as for the LDA case, it is important to choose the correct value for the screening charge. As both HF and CCSD(T) are self-interaction free, we expect $Q_{scr} = N - 1$. Unlike in the LDA case, there is no way of determining if this is the exact numeric value; however, our results strongly suggest that this is a good choice. We again focus on the IPs obtained from the HOMO orbital energies to judge the quality of our inversion procedure. For HF-inverted densities, by Koopmans' theorem[55] and its analogue in DFT relating the HOMO energy to the IP,[49] we expect the inverted ϵ_H to equal ϵ_H from HF. Meanwhile, for the densities inverted from CCSD(T), the difference in the IP compared to experiment should offer insight into the reliability of the procedure.

In Table IV, we see how the IPs taken from the HOMO energies of the inverted local potential compared with the IPs from HF theory. These results indicate what level of accuracy can be expected with a given basis set: it appears we should use at least cc-pVTZ basis sets to obtain an accurate potential, with an average difference of 3.4% between the inverted and actual IPs. More accurate results can be obtained if desired by increasing the basis set size. A similar picture emerges for the inverted CCSD(T) densities, as seen in Table V; in this case, cc-pVQZ results are not computed at the expense of obtaining the coupled cluster density matrix for these densities, but we see a very similar result for the average error in cc-pVTZ basis sets.

Besides these IP comparisons, we demonstrate the applicability of our method by plotting some xc-potentials. In Fig. 3, we see that

TABLE V. Comparison of IPs for the local potential of a CCSD(T) density with experimental IPs.

	cc-pVDZ		cc-pVTZ		
IP (ev)	Inverse	% err.	Inverse	% err.	Expt.[50]
He	24.94	1.4	24.57	0.1	24.59
Be	9.13	2.0	9.12	2.0	9.32
Ne	12.09	43.9	20.41	5.3	21.56
HF	11.34	29.3	15.43	3.7	16.03
H_2O	10.01	20.7	12.28	2.7	12.62
H_2	15.91	3.1	16.45	6.6	15.43
CO	10.01	28.6	13.18	5.9	14.01
Avg % err.	...	18.4	...	3.8	...

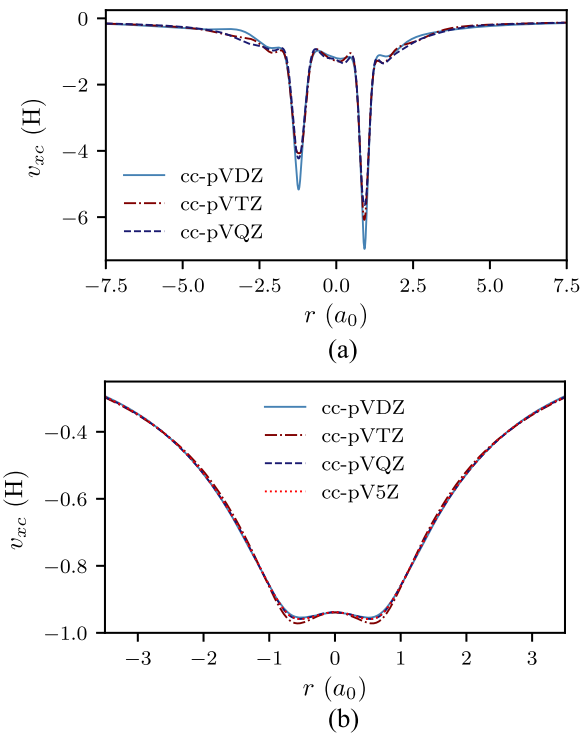

FIG. 3. xc-Potentials for (a) the inverted HF density of CO and (b) the inverted CCSD(T) density of H_2 for various basis sets.

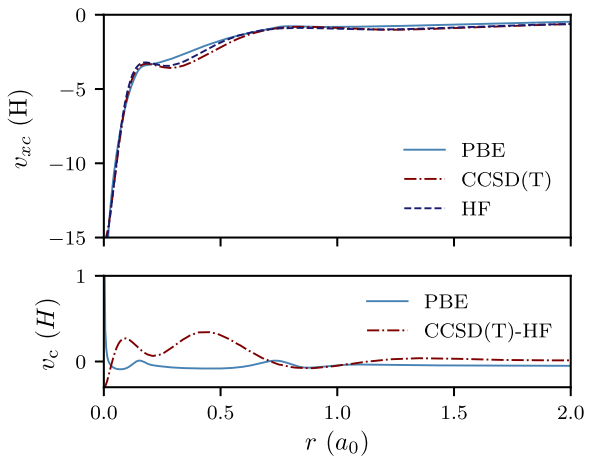

FIG. 4. Top: Ar (cc-pvTZ) xc-potentials from inverted HF and CCSD(T) densities, and PBE; bottom: correlation potentials from the difference of CCSD(T) and HF inverted xc-potentials, and PBE.

the xc-potentials converge with the basis set and produce smooth potentials. As in the LDA case, the inversion procedure struggles most in the regions very close to the nuclei. However, the inverted potentials appear to converge well for the purposes of qualitative analysis outside of these regions.

We can also obtain approximate correlation potentials by taking the difference between the (almost) fully correlated inverted CCSD(T) potential and the exchange-only inverted HF potential. We can expect this to yield accurate correlation potentials when the system under consideration is weakly correlated, as in this case the inverted HF potential is close to the exact-exchange potential.[29,53] In Fig. 4, we have plotted this correlation potential and the xc-potential for argon, along with a comparison with the Perdew-Burke-Ernzerhof (PBE) potential.[56]

IV. COMPARISON WITH THE METHOD BY ZHAO, MORRISON, AND PARR

Zhao, Morrison, and Parr (ZMP), in their well-known density-inversion method,[19] impose the constraint that the Coulomb energy $U[\rho - \rho_t]$ (1) actually vanishes, rather than be minimized. The KS potential in their method

$$v_s^{\Lambda}(\mathbf{r}) = v_{\text{en}}(\mathbf{r}) + \left(1 - \frac{1}{N}\right) v_{\text{H}}[\rho](\mathbf{r}) + \Lambda \int d\mathbf{r}' \, \frac{\rho(\mathbf{r}') - \rho_t(\mathbf{r}')}{|\mathbf{r} - \mathbf{r}'|} \quad (22)$$

consists of the external potential $v_{\text{en}}(\mathbf{r})$, the Fermi–Amaldi potential $(1 - 1/N)\, v_{\text{H}}[\rho](\mathbf{r})$, with $v_{\text{H}}[\rho](\mathbf{r})$ the Hartree potential, and finally, an effective potential to satisfy the constraint of zero $U[\rho - \rho_t]$, in the limit of the diverging Lagrange multiplier $\Lambda \to \infty$. ZMP argue that inclusion of the Fermi–Amaldi potential in their KS potential is auxiliary, to aid convergence and relieve the burden of the xc-potential when Λ is finite. However, at any finite Λ, inclusion of the Fermi–Amaldi potential in (22) is crucial since it is the term that provides the correct screening charge required by the target density. Its omission would imply that in the asymptotic region, a KS electron would be attracted by the full, unscreened nuclear charge. See also the discussion by Liu, Ayers, and Parr in Ref. 34.

The connection and similarity between the method by ZMP and ours is analogous to the connection between the direct minimization of a total energy density functional and its indirect minimization using the optimized effective potential (OEP) method.[57,58] The ZMP KS equations can be derived by the direct minimization of the standard DFT total energy expression (as a density functional), using $E_{\text{xc}}^{\text{ZMP}}[\rho] = \Lambda U[\rho - \rho_t] - (1/N) U[\rho]$ in place of the "xc" energy density functional. The total energy minimization must then be carried out for various values of Λ and the results extrapolated to $\Lambda \to \infty$. The analogy with our method is that we work only with $\Lambda = \infty$ and rather than the whole total energy, we minimize just $U[\rho - \rho_t]$. Only then, $U[\rho - \rho_t]$ becomes a functional of the effective potential $v_{\text{en}} + v$ that yields ρ, i.e., $\rho = \rho_v$, and $U[\rho_v - \rho_t]$ must be minimized with the OEP method.

V. DISCUSSION

We have presented a reliable inversion method to find the local KS potential corresponding to the given target density. This method utilizes the concept of a screening density, which offers controlling the minimization procedure to yield physical potentials and also aids our understanding of self-interactions in DFT.

The steepest descent method presented here is a stable method to invert the density and works well for large enough basis sets for atoms and molecules at their equilibrium geometries. Work is in progress to improve convergence for more complicated input densities (such as for stretched molecules) and will be presented in a future publication.

ACKNOWLEDGMENTS

N.I.G. acknowledges financial support by the Leverhulme Trust, through a research project grant (No. RPG-2016-005).

N.N.L. acknowledges support by the project "Advanced Materials and Devices" (Grant No. MIS 5002409) funded by NSRF 2014–2020.

T.J.C. and N.I.G. thank Professor Rod Bartlett for very helpful discussions during his visit at Durham University in early 2019 and acknowledge the Institute of Advanced Study at Durham University for hosting this visit.

DATA AVAILABILITY

The data that support the findings of this study can be obtained from the corresponding author upon reasonable request.

APPENDIX A: CHOICE OF BASIS SET REPRESENTATION FOR ρ_{scr}

As discussed in Sec. II A, we expand the screening density in an auxiliary basis set, which is the density-fitted set corresponding to the orbital basis. This is an intuitive choice because we represent an effective density with a basis set designed for densities; it is also a convenient choice because density-fitted sets are frequently used anyway to accelerate the computation of integrals in quantum chemistry codes.[59,60]

To justify this choice quantitatively, we recall that we can directly obtain the Gaussian representation of the LDA grid

TABLE VI. Values of $U[\rho_{ga} - \rho_{gr}]$ for LDA potentials in different Gaussian basis sets. All bases are cc-pVTZ.

$U[\rho_{ga} - \rho_{gr}]$	Orbital	Uncontracted	ρ-fitted
He	2.3×10^{-7}	2.1×10^{-7}	1.2×10^{-8}
Be	7.0×10^{-4}	5.5×10^{-9}	4.2×10^{-10}
Ne	9.0×10^{-5}	1.8×10^{-6}	3.4×10^{-10}
HF	9.0×10^{-5}	2.9×10^{-7}	7.5×10^{-9}
H_2O	1.2×10^{-4}	2.2×10^{-7}	8.5×10^{-9}
H_2	7.0×10^{-8}	1.6×10^{-7}	6.0×10^{-8}
CO	3.5×10^{-4}	2.7×10^{-7}	1.6×10^{-9}

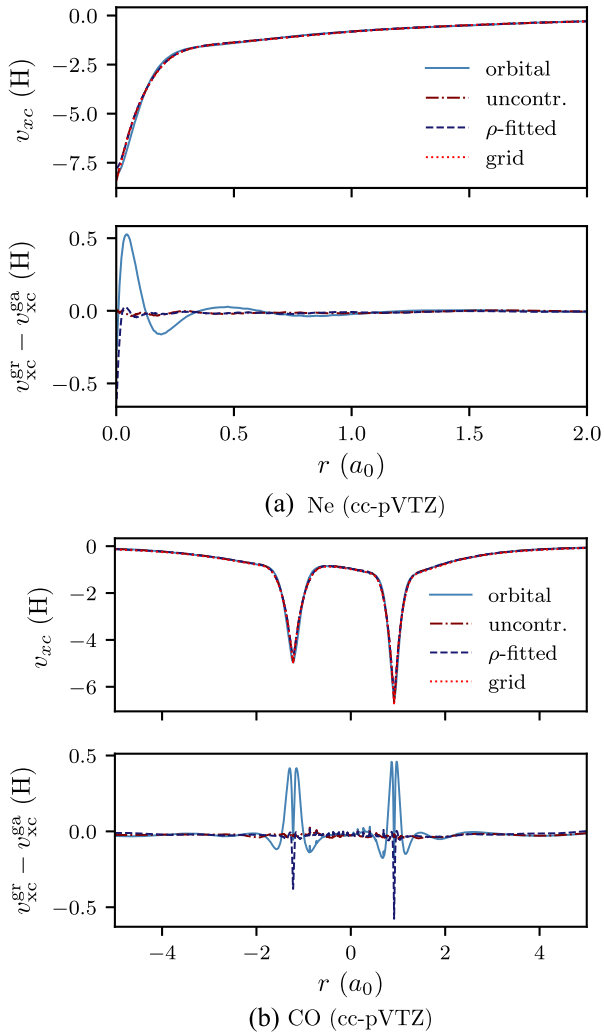

FIG. 5. Comparison of the LDA xc-potential on a grid, against various Gaussian basis set representations. Lower images show the differences between the grid and Gaussian representation.

potential using Eq. (18). As a measure to gauge the quality of defining the potential in a given basis set, we use the Coulomb energy $U[\rho_{ga} - \rho_{gr}]$ (1), where ρ_{ga} and ρ_{gr} are the densities arising from defining the potential in a Gaussian basis set and on the grid respectively. The smaller the value of $U[\rho_{ga} - \rho_{gr}]$, the better one might expect the Gaussian representation to be. In Table VI, we compare the values of $U[\rho_{ga} - \rho_{gr}]$ for three choices of basis functions for the screening density: the orbital basis, the density-fitted basis, and the uncontracted orbital basis, which is a common choice for the potential.[6,33] We observe that the density-fitted sets give the closest fit to the grid representation based on this criterion.

In Fig. 5, we plot the LDA xc-potentials for these basis set choices. In contrast to the above-mentioned analysis, the uncontracted sets seem to give the best fit to the grid potential, but we note that the density-fitted sets give a close fit everywhere except the nuclear positions. In our experience, the algorithm works more smoothly for the density-fitted sets than the uncontracted ones. Given that we minimize $U[\rho_v - \rho_t]$, it makes sense to choose a representation that also minimizes this expression. The gradient-descent algorithm also struggles to reproduce the target density near the nuclei regardless of the auxiliary basis chosen, so the lack of accuracy of the density-fitted sets in this region is not so important in our method.

APPENDIX B: CONVERGENCE CRITERIA

The convergence criteria for the objective functional U and the change in objective functional δU were set to 5×10^{-9} hartree and 5×10^{-11} hartree per electron, respectively. If both of these conditions are satisfied, U is taken to be converged.

In general, satisfying the above criteria is not a problem when inverting a DFT density (e.g. LDA). However, when inverting non-local densities, the problem of spurious oscillations tends to emerge and thus it is necessary to use a regularization criterion. As mentioned in Sec. II A, we monitor the amount of negative screening charge to indicate the onset of these spurious oscillations.

The onset of negative screening charge is dependent on several factors, including

i. the number of electrons N,
ii. the size of the basis set, and
iii. the target density,

and other (hard to quantify) factors relating to the system under consideration. To guide our intuition, we use the procedure outlined in Sec. III A to determine the behavior of the "exact" $\rho_s(\mathbf{r})$ for LDA densities.

In Table VII, we see that a small amount of negative screening charge is typically present for the LDA effective screening density. In Fig. 6, we see this negative screening density has a tendency to build up near the nuclei. There is no reason to expect a dramatically dissimilar behavior for different target densities, and therefore, it seems judicious to allow a small amount of negative screening charge to manifest itself in the inversion procedure. However, as previously discussed, if Q_{neg} is permitted to increase too fast or become too large, then we observe the onset of undesirable oscillations in the potential.

TABLE VII. Amount of negative screening charge, Q_{neg}, for exact LDA screening densities.

Q_{neg}	cc-pVDZ	cc-pVTZ
He	0.0	9.88×10^{-3}
Be	5.81×10^{-2}	7.65×10^{-2}
Ne	0.0	3.3×10^{-4}
HF	4.5×10^{-2}	8.18×10^{-2}
H_2O	3.03×10^{-2}	1.15×10^{-1}
H_2	6.55×10^{-3}	6.35×10^{-2}
CO	1.09×10^{-2}	3.51×10^{-4}

With the above-mentioned arguments in mind, we monitor the following variables during the inversion procedure:

i. soft limit, Q_{neg}^{soft};
ii. change in Q_{neg}, δQ_{neg} between iterations;
iii. hard limit, Q_{neg}^{hard}.

If both conditions (i) and (ii) are satisfied, or if just condition (iii) is satisfied, the calculation stops. For all the results published in this paper, we use the same values, which are equal to

i. $Q_{neg}^{soft} = 0.01$,
ii. $\delta Q_{neg} = 0.005$, and
iii. $Q_{neg}^{hard} = 0.05$,

where all the above values are quoted per electron. These values give reasonable results for the systems presented in this paper, which are all atoms or molecules at their equilibrium geometries. However, we have observed that for molecules stretched beyond their equilibrium geometries, a large build-up of negative screening charge develops. A more sophisticated procedure would be required for these and other difficult cases.

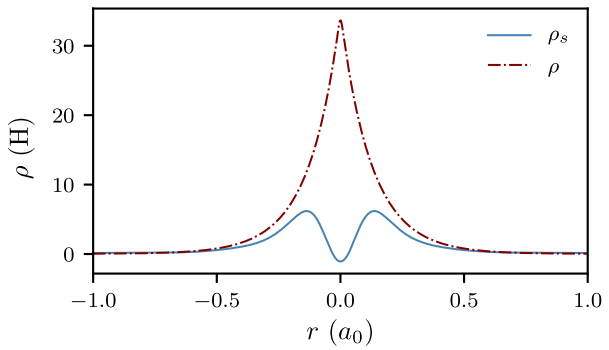

(a) Be (cc-pVTZ)

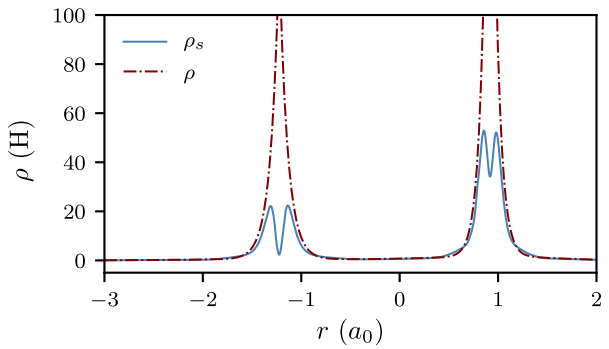

(b) CO (cc-pVTZ)

FIG. 6. Effective screening densities, $\rho_s(\mathbf{r})$, for LDA densities, with the actual densities for comparison. We observe the tendency for a small amount of negative screening charge near the nuclei.

REFERENCES

[1] A. Pribram-Jones, D. A. Gross, and K. Burke, Annu. Rev. Phys. Chem. **66**, 283 (2015).
[2] A. J. Cohen, P. Mori-Sanchez, and W. Yang, Science **321**, 792 (2008).
[3] N. T. Maitra, J. Phys.: Condens. Matter **29**, 423001 (2017).
[4] J. Sun, A. Ruzsinszky, and J. P. Perdew, Phys. Rev. Lett. **115**, 036402 (2015).
[5] A. Thierbach, D. Schmidtel, and A. Görling, J. Chem. Phys. **151**, 144117 (2019).
[6] T. Pitts, N. I. Gidopoulos, and N. N. Lathiotakis, Eur. Phys. J. B **91**, 130 (2018).
[7] R. J. Bartlett, J. Chem. Phys. **151**, 160901 (2019).
[8] C. Li, X. Zheng, A. J. Cohen, P. Mori-Sánchez, and W. Yang, Phys. Rev. Lett. **114**, 053001 (2015).
[9] M.-C. Kim, H. Park, S. Son, E. Sim, and K. Burke, J. Phys. Chem. Lett. **6**, 3802 (2015).
[10] C. O. Almbladh and A. C. Pedroza, Phys. Rev. A **29**, 2322 (1984).
[11] F. Aryasetiawan and M. J. Stott, Phys. Rev. B **38**, 2974 (1988).
[12] A. Nagy and N. H. March, Phys. Rev. A **39**, 5512 (1989).
[13] Á. Nagy and N. H. March, Phys. Rev. A **40**, 554 (1989).
[14] A. Nagy, J. Phys. B: At., Mol. Opt. Phys. **26**, 43 (1993).
[15] A. Nagy, Philos. Mag. B **69**, 779 (1994).
[16] J. Chen, R. O. Esquivel, and M. J. Stott, Philos. Mag. B **69**, 1001 (1994).
[17] S. H. Werden and E. E. Davidson, in *Local Density Approximations in Quantum Chemistry and Solid State Physics*, 1st ed., edited by J. P. Dahl and J. Avery (Plenum, New York, 1984), Chap. III, pp. 33–42.
[18] Y. Wang and R. G. Parr, Phys. Rev. A **47**, R1591 (1993).
[19] Q. Zhao, R. C. Morrison, and R. G. Parr, Phys. Rev. A **50**, 2138 (1994).
[20] A. Görling, Phys. Rev. A **46**, 3753 (1992).
[21] Q. Wu and W. Yang, J. Chem. Phys. **118**, 2498 (2003).
[22] R. van Leeuwen and E. J. Baerends, Phys. Rev. A **49**, 2421 (1994).
[23] A. Kumar, R. Singh, and M. K. Harbola, J. Phys. B: At., Mol. Opt. Phys. **52**, 075007 (2019).
[24] B. Kanungo, P. M. Zimmerman, and V. Gavini, Nat. Commun. **10**, 4497 (2019).
[25] M. J. P. Hodgson, J. D. Ramsden, J. B. J. Chapman, P. Lillystone, and R. W. Godby, Phys. Rev. B **88**, 241102 (2013).
[26] S. E. B. Nielsen, M. Ruggenthaler, and R. van Leeuwen, Europhys. Lett. **101**, 33001 (2013).
[27] D. S. Jensen and A. Wasserman, Phys. Chem. Chem. Phys. **18**, 21079 (2016).
[28] D. S. Jensen and A. Wasserman, Int. J. Quantum Chem. **118**, e25425 (2018).
[29] T. W. Hollins, S. J. Clark, K. Refson, and N. I. Gidopoulos, J. Phys.: Condens. Matter **29**, 04LT01 (2016).
[30] A subtle point is that, in general, v is not exactly equal to the Hxc potential of the KS system with density ρ_v. Since v_{en} is the external potential for the KS system with density ρ_t, it cannot also be the external potential for the KS system with density ρ_v. Hence, as long as $\rho_v \neq \rho_t$, the potential v is not exactly equal to the Hxc potential of the KS system with density ρ_v.
[31] N. I. Gidopoulos, Phys. Rev. A **83**, 040502 (2011).
[32] N. I. Gidopoulos and N. N. Lathiotakis, J. Chem. Phys. **136**, 224109 (2012).
[33] A. Görling, Phys. Rev. Lett. **83**, 5459 (1999).
[34] S. Liu, P. W. Ayers, and R. G. Parr, J. Chem. Phys. **111**, 6197 (1999).
[35] P. Mori-Sánchez, A. J. Cohen, and W. Yang, J. Chem. Phys. **125**, 201102 (2006).

[36]For information, contact NL at lathiot@eie.gr.
[37]F. Weigend, A. Köhn, and C. Hättig, J. Chem. Phys. **116**, 3175 (2002).
[38]F. A. Bulat, T. Heaton-Burgess, A. J. Cohen, and W. Yang, J. Chem. Phys. **127**, 174101 (2007).
[39]S. Hirata, S. Ivanov, I. Grabowski, R. J. Bartlett, K. Burke, and J. D. Talman, J. Chem. Phys. **115**, 1635 (2001).
[40]V. N. Staroverov, G. E. Scuseria, and E. R. Davidson, J. Chem. Phys. **124**, 141103 (2006).
[41]N. I. Gidopoulos and N. N. Lathiotakis, Phys. Rev. A **85**, 052508 (2012).
[42]M. Levy, Proc. Natl. Acad. Sci. U. S. A. **76**, 6062 (1979).
[43]W. Kohn, Phys. Rev. Lett. **51**, 1596 (1983).
[44]J. Chen and M. J. Stott, Phys. Rev. A **44**, 2816 (1991).
[45]J. Chen and M. J. Stott, Phys. Rev. A **47**, 153 (1993).
[46]A. Schindlmayr and R. W. Godby, Phys. Rev. B **51**, 10427 (1995).
[47]M. Däne and A. Gonis, Computation **4**, 24 (2016).
[48]B. P. Pritchard, D. Altarawy, B. Didier, T. D. Gibson, and T. L. Windus, J. Chem. Inf. Model. **59**, 4814 (2019).
[49]J. P. Perdew, R. G. Parr, M. Levy, and J. L. Balduz, Phys. Rev. Lett. **49**, 1691 (1982).
[50]S. G. Lias, in *NIST Chemistry WebBook*, NIST Standard Reference Database Number 69, edited by P. Linstrom and W. Mallard (National Institute of Standards and Technology, Gaithersburg, MD, 2018).
[51]R. M. Parrish, L. A. Burns, D. G. A. Smith, A. C. Simmonett, A. E. DePrince, E. G. Hohenstein, U. Bozkaya, A. Y. Sokolov, R. Di Remigio, R. M. Richard, J. F. Gonthier, A. M. James, H. R. McAlexander, A. Kumar, M. Saitow, X. Wang, B. P. Pritchard, P. Verma, H. F. Schaefer, K. Patkowski, R. A. King, E. F. Valeev, F. A. Evangelista, J. M. Turney, T. D. Crawford, and C. D. Sherrill, J. Chem. Theory Comput. **13**, 3185 (2017).
[52]U. Bozkaya and C. D. Sherrill, J. Chem. Phys. **147**, 044104 (2017).
[53]V. N. Staroverov, G. E. Scuseria, and E. R. Davidson, J. Chem. Phys. **125**, 081104 (2006).
[54]T. D. Crawford and H. F. Schaefer, Rev. Comput. Chem. **14**, 33 (2000).
[55]T. Koopmans, Physica **1**, 104 (1934).
[56]J. P. Perdew, K. Burke, and M. Ernzerhof, Phys. Rev. Lett. **77**, 3865 (1996).
[57]R. T. Sharp and G. K. Horton, Phys. Rev. **90**, 317 (1953).
[58]J. D. Talman and W. F. Shadwick, Phys. Rev. A **14**, 36 (1976).
[59]E. J. Baerends, D. E. Ellis, and P. Ros, Chem. Phys. **2**, 41 (1973).
[60]K. Eichkorn, O. Treutler, H. Öhm, M. Häser, and R. Ahlrichs, Chem. Phys. Lett. **242**, 652 (1995).
[61]M. W. Schmidt, K. K. Baldridge, J. A. Boatz, S. T. Elbert, M. S. Gordon, J. H. Jensen, S. Koseki, N. Matsunaga, K. A. Nguyen, S. Su, T. L. Windus, M. Dupuis, and J. A. Montgomery, Jr., J. Comput. Chem. **14**, 1347 (1993).
[62]M. S. Gordon and M. W. Schmidt, in *Theory and Applications of Computational Chemistry*, edited by C. E. Dykstra, G. Frenking, K. S. Kim, and G. E. Scuseria (Elsevier, Amsterdam, 2005), pp. 1167–1189.